

Pedestrian Level Wind Environment around Isolated Buildings Resulted from Twisted Wind Profiles

X. Zhang¹, A.U. Weerasuriya¹, K.T. Tse¹ and K.C.S. Kwok²

¹Department of Civil and Environmental Engineering
Hong Kong University of Science and Technology, Hong Kong, China

²Institute for Infrastructure Engineering
University of Western Sydney, Penrith, NSW, 2751, Australia

Abstract

The pedestrian-level wind environment influenced by twisted wind profiles were evaluated through a series of wind tunnel tests. In the tests, more than 200 Irwin sensors were installed to measure the wind speeds at pedestrian level around five isolated buildings, each with different dimensions. Two twisted wind profiles, with a maximum twist angle of 13° and 22° respectively, were simulated in a boundary-layer wind tunnel. A conventional log-law type turbulent boundary layer profile was employed to repeat the wind tunnel test to act as a control case. Based on the wind speeds measurements, the velocity ratios (VR) were calculated to show the influence of the twisted profiles. By comparing the VR distributions under the influence of the two twisted profiles to the VR distributions in the conventional wind profile, it is observed that (a) the VR distribution in the wake zone is skewed according to the maximum twisted angle, (b) the over-speed area ($VR > 1.2$) decreases and the shelter area ($VR < 0.8$) increases in the pedestrian-level wind field under the influence of the twisted profiles.

Introduction

Pedestrian-level wind field is of great importance from various perspectives. For example, unpleasant high-speed winds may lead to a discomfort environment for pedestrians, and the weak wind zone could be ineffectual for air pollutant dispersions. It is well-established that the pedestrian-level wind field in city centres are significantly influenced by the building shapes. Evidently, the undesirable air ventilation conditions in the urban areas of mega-cities such as Hong Kong are attributable to the compact arrangement for high-rise buildings commonly found in those mega-cities. Therefore, an accurate and reliable estimation of the influence of building shapes on the pedestrian-level wind field is important for authorities to prevent unpleasant conditions for pedestrians and to enhance the living conditions for urban inhabitants. Considering the size and the population, cities like Hong Kong demand more sophisticated regulations to ensure both pedestrian comfort and urban air ventilations are adequately addressed.

Since the outbreak of Severe Acute Respiratory Syndrome (SARS) in 2003, the Hong Kong government has been actively investigating the possibility to implement a mandatory test, called Air Ventilation Assessment (AVA), for any commercial and residential developments occurred in Hong Kong. Indeed, AVA is now required for all land developments initiated by the public sector. As an important component of the AVA methodology, wind tunnel model tests are required to be carried out to determine the influence of the proposed development on the pedestrian-level wind field around the site. Understandably, the success of the implementation of the AVA depends, to a large extent, on the accuracy of the wind tunnel measurements of the pedestrian-level wind field.

As a deterministic part of any wind tunnel test, the simulation of the approaching wind flow significantly impacts the overall reliability of the wind tunnel test and the accuracy of the test results. For buildings constructed in Hong Kong, the approaching wind flow is often modulated by complex terrain topographies. It has been frequently found that the wind flow approaching the buildings in the harbour area of Hong Kong deviates from a conventional turbulent boundary layer profile simulated in the wind tunnel. In particular, the wind direction has been found to vary significantly vertically in the wake of a hill. In the course of assessing the micro wind environment at various areas in Hong Kong, 18 AVA wind tunnel tests have been conducted in the boundary-layer wind tunnel at Hong Kong University of Science and Technology's CLP Power Wind/Wave Tunnel Facility. Among 256 wind profiles measured in the 18 tests, 45% exhibit a wind direction difference (between profile top and bottom) larger than 8°, and 21% show a wind direction difference larger than 15°. Since the wind direction difference, which is referred to as twisting effect hereafter, is generally confined to the lower 300m, it is expected that the twisting effect will significantly influence the pedestrian-level wind field. Consequently, it is necessary to include the twisting effect in a wind tunnel test to assess the pedestrian-level wind field around new developments, particularly those situated in the immediate vicinity of significant topographical features. A long-term project has been initiated to develop an engineering model to describe the influence of the twisting effect on the pedestrian-level wind field quantitatively. As a first step, it is necessary to understand the similarities and differences of the pedestrian-level wind fields under the influence of different approaching wind flows: a conventional turbulent boundary layer profile, and profiles with different twisting effects, referred to as twisted profile hereafter.

Due to technical challenges, there are few studies concerning the influence of the twisting effect on the aerodynamics of downstream objects. Flay and his co-workers (Flay, 1996; Richards et al., 1996) conducted both wind tunnel and numerical simulations using the twisted wind profile to evaluate the performance of downwind yacht's sail. It is noteworthy that their results highlighted the importance of employing a more realistic twisted profile to calibrate the approaching wind flow in both the wind tunnel and numerical simulations.

Given the fact that the twisting effect is commonly observed in the wind field around Hong Kong and the impact of the approaching wind flow on wind tunnel model studies, this paper discusses the influence of the twisting effect on the pedestrian-level wind field by comparing the wind speed measurements taken in the wind tunnel tests under the influence of the conventional turbulent boundary layer profile and twisted approaching wind profiles. The discussion is mainly focused on the similarities and differences between the pedestrian-level wind fields measured in two sets of wind tunnel model tests.

Experimental setup

All the wind tunnel model tests described in this paper were conducted in the low wind speed section of the boundary layer wind tunnel at Hong Kong University of Science and Technology's CLP Power Wind/wave Tunnel Facility. The test section is 5m in width and 4m in height with a maximum wind speed of 10 m/s. Two twisted profiles, namely TWP13 and TWP22, with a maximum wind direction difference of 13° and 22° respectively were simulated. The twisted profiles were generated using a vane systems installed 4m upstream the turntable centre. The vertical variation of wind directions were measured throughout the test section to identify an area in which the desired twisting effect is sustained for some distances. It was found that an area, whose centre is 0.5m downstream of the turntable centre, with dimensions of 3m × 2m, has wind profiles showing consistent characteristics. Regularly arranged roughness elements were installed in the upstream fetch to simulate the turbulent boundary layer profile, which is a commonly adopted approach for conventional wind tunnel tests. The normalized mean wind speed and turbulence intensity profiles in the approaching wind flow of the conventional turbulent boundary layer profile and the twisted wind profiles are shown in Figure 1 (a). The vertical variation of the wind direction measured at the turntable centre is shown in Figure 1(b). It should be noted the vane system was designed to modulate the vertical variation of the wind direction follows a negative power-law curve.

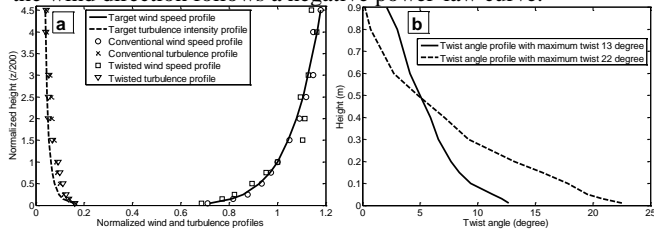


Figure 1. (a) Normalized mean wind and turbulence intensity profiles used for pedestrian level wind tunnel test, (b) Twisted angle profiles at centre of turntable.

Pedestrian-level wind speeds were measured by using Irwin sensors, which are essentially omni-directional pressure sensors. Irwin sensors have used in many studies with similar settings (e.g. Irwin, 1981; Wu and Statopolous, 1994, Tsang, 2012). The Irwin sensors used in the present study are similar to those used by Tsang (2012) with 10mm high protrude tube as shown in Figure 2(a). Due to the geometric scale of 1:200, 10 mm in the wind tunnel scale represents 2m pedestrian height in the prototype scale. Around 200 Irwin sensors were arranged in a rectangular grid covering an area of 100mm × 75mm, as shown in Figure 2(b). It should be noted that the grid spacing becomes larger farther downstream of the test building due to the limitation of the number of connections available and the stability of the pressure scanner. The measurements were taken for 120 seconds at a sampling frequency of 500 Hz. In addition to the Irwin sensor measurements, a hot wire anemometer was installed to measure the reference wind speeds. The reference point was located upstream of the test building. The sampling frequency and period were the same as the Irwin sensor measurements. A photograph showing the experimental set-up is given in Figure 3.

Model	Dimensions (H×W×D) (mm)	Aspect ratio (H/W)
M1	600×150×100	4:1
M2	300×150×100	2:1
M3	225×150×100	1.5:1
M4	225×300×100	0.75:1
M5	225×450×100	0.50:1

Table 1. Building dimensions and aspect ratios of five isolated building models.

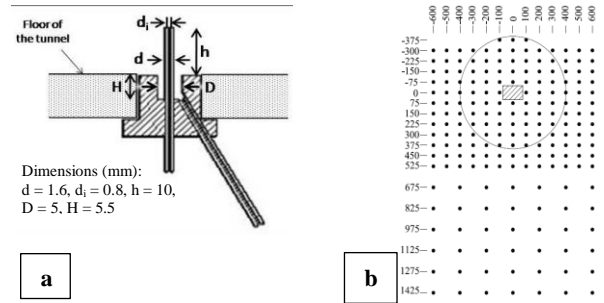


Figure 2. (a) Dimensions of Irwin sensor, (b) Arrangement of Irwin sensors (dimensions in mm).



Figure 3. Building model and vane system set up in low wind speed section of boundary layer wind tunnel.

At the turntable centre, 5 isolated building models were tested in sequence. Table 1 summarizes the building model dimensions: H = building height, W = building width, D = building depth = length of the building in the along-wind direction.

Results

The results of pedestrian-level wind tunnel tests are presented as contours of velocity ratios (VR). The velocity ratio is defined as

$$VR = \frac{\bar{V}(x, 1p)}{V_a(x, 1p)} \quad (1)$$

$\bar{V}(x, 10)$ is the mean wind velocity measured with the test building in place at 10mm above ground at grid point x . $\bar{V}_a(x, 10)$

is the mean wind velocity at the exact same location without the test building. Although wind gusts are derivable from the Irwin sensor measurements, only the mean wind velocity is presented in this paper. The contours of VRs around three isolated building models with the same width but different heights (i.e. Models: M1, M2, and M3) under the influence of the three approaching wind profiles (one conventional turbulent boundary layer profile and two twisted profiles) are displayed in Figure 4 (a) to (i).

Regardless of the approaching profile, common features were identified in the pedestrian-level wind field around all the building models tested, as shown in Figure 5 (a). Specifically, there are four low wind speed zones in the upstream direction near the building (UNLWS), in the upstream direction far from the building (UFLWS), in the downstream direction near the building (DNLWS) and in the downstream direction far from the building (DFLWS). Additionally, there is a high speed zone in the corner streams (CS).

By comparing the contours shown in Figure 4, it is observed that the DFLWS deviates from the exact downstream direction (defined according to the building section) along with an increase in the twisted angle. For the pedestrian-level wind field under the influence of the turbulent boundary layer profile, the DFLWS lies right behind the building model. For the pedestrian-level wind fields under the influence of the twisted profiles, the DFLWS, however, shifts according to the wind attack angle near the

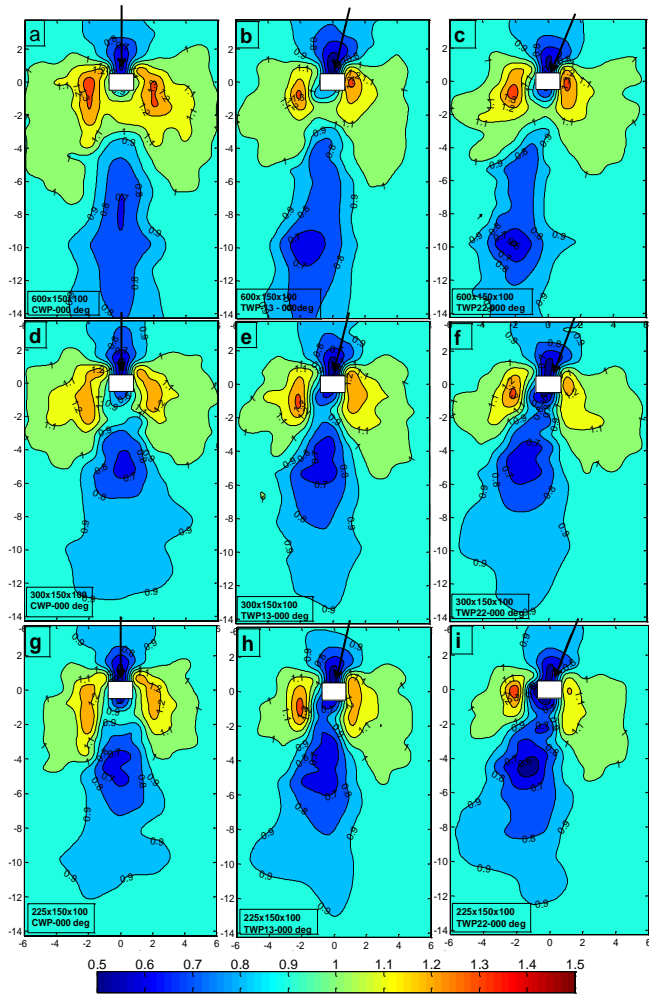


Figure 4. Wind speed ratio distribution at 10 mm above ground around (a) 600×150×100 building with CWP, (b) 600×150×100 building with TWP13, (c) 600×150×100 building with TWP22, (d) 300×150×100 building with CWP, (e) 300×150×100 building with TWP13, (f) 300×150×100 building with TWP22, (g) 225×150×100 building with CWP, (h) 225×150×100 building with TWP13, (i) 225×150×100 building with TWP22.

ground. If the angle by which the DFLWS shifts from the exact downstream direction is defined as the deviation of the DFLWS (shown in Figure 5(b)), it was found that the DFLWS deviation increases with the maximum twisted angle in the approaching wind profile. The size of the DFLWS, in addition, increases with the maximum twisted angle. In other words, the blocking effect of the building is more obvious in the twisted wind flow than in the conventional turbulent boundary layer wind flow. When the pedestrian-level wind field under the influence of the twisted approaching wind profile is rotated according to the near-surface wind attack angle, it was found that the DFLWS is still approximately symmetrical about the vector showing the wind flow attacking the building model. In addition to the low speed zones, the locations of the high speed zones (CS) were shifted with the change of the approaching wind profile from the conventional turbulent boundary layer profile to the twisted profile. In particular, the corner stream at the left side was found to be stronger than at the right side in the twisted-profile-influenced wind field. This is probably due to the near-surface wind flow attacks the building from the left side although the aloft wind flow approaches the front face of the building model. By comparing Figures 4 (d)-(i), it is clear that the height of the building has noticeable impacts on how the twisting effect influences the pedestrian-level wind field. Evidently, the twisting effect has more significant impacts when the building model is

shorter (building height is reduced). Regardless of the approaching wind profile, the DFLWS zone moves towards the building when the building height is reduced. The DFLWS deviation, however, is merely influenced by the move of the DFLWS. In other words, the DFLWS deviation roughly keeps constant when the building height varies. Therefore, it is concluded that the twisting effect has more obvious impacts on the distribution of VRs, and hence the pedestrian-level wind field.

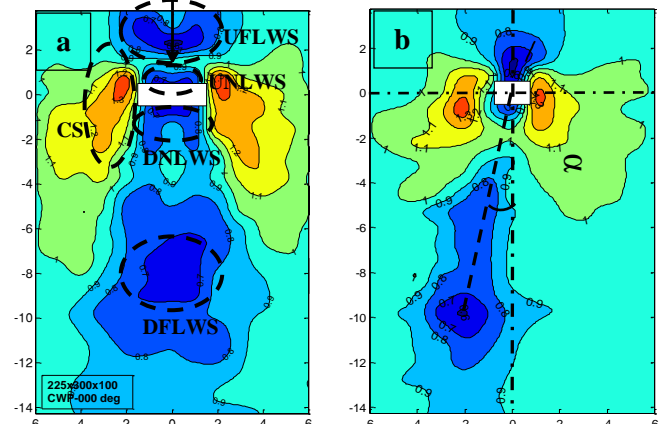


Figure 5. (a) over speed and sheltered area around an isolated building model, (b) Definition of deviated angle (α) of UFLWS.

Figures 6 (a) to (i) illustrate VR distribution under the influence of the three approaching profiles around three building models; M3, M4 and M5. From Table 1, M3, M4 and M5 share the building height but have different building widths. The DNLWS area grows with an increase of the building width due to blocking effect enhancement. The DFLWS zone, on the other hand, increases in sizes and moves further downstream with an increase of the building width. In contrast to the pedestrian-level wind field around a taller building, such as M1, UFLWS zones are visible in Figures 6 (d)-(i). It is worth noting that, even for building M1, UFLWS is not entirely absent but remains outside of the measurement area. The maximum wind speed at the corner streams become smaller in the wind field around a wider building because of the weaker downwash occurred at the windward side of the buildings.

From Table 2, it is clear that deviation of DFLWS is not significantly influenced by the building height. The building width, on the other hand, drives the DFLWS deviation to increase. The increase in DFLWS deviation in the wind field under the influence of the twisted profile with the maximum twisted angle of 13° is, however, not significant. The position of the DFLWS moves further away with the increase of the maximum twisted angle and the width of the building.

One of the aims for the present study is to investigate the similarities and differences in the pedestrian-level wind field under the influence of the conventional and twisted approaching wind profile. As a generalised measure of the characteristics of the pedestrian-level wind field, the over-speed area (defined as $VR > 1.2$) and the sheltered area (defined as $VR < 0.8$) are identified based on the wind tunnel measurements taken in the wind tunnel tests. In this study, the over-speed criterion corresponds to an actual wind speed greater than 5 m/s and the sheltered area has wind speeds less than 3 m/s. When the over-speed and sheltered areas are expressed as percentages with respect to entire sensor coverage area, Figures 7(a) and (b) display the variation of the percentage with the model selection. Figure 7(a) indicates that the over-speed area corresponding to the conventional turbulent boundary layer profile and the twisted profile with a maximum twisted angle of 13° are roughly the same. The over-speed area corresponding to the twisted profile with a maximum twisted angle of 22°, on the other hand, is

smaller. The over-speed area increases with increasing building height and width, which generally agrees with the findings made in previous studies conducted in conventional turbulent boundary layer approaching wind profile. The twisting effect slows down the increase of the over-speed area with the increase of the building width. This is probably due to the lower corner stream wind speed observed at the right side of the building in the twisted wind flow. The shelter area, on the other hand, increases with the maximum twisted angle. While the increase is not obvious in the wind field around tall buildings, it becomes prominent for wide and short buildings. This is attributable to the increase in blocking effect when the vertical variation of wind directions interacted with not only the front but also the side faces of the building.

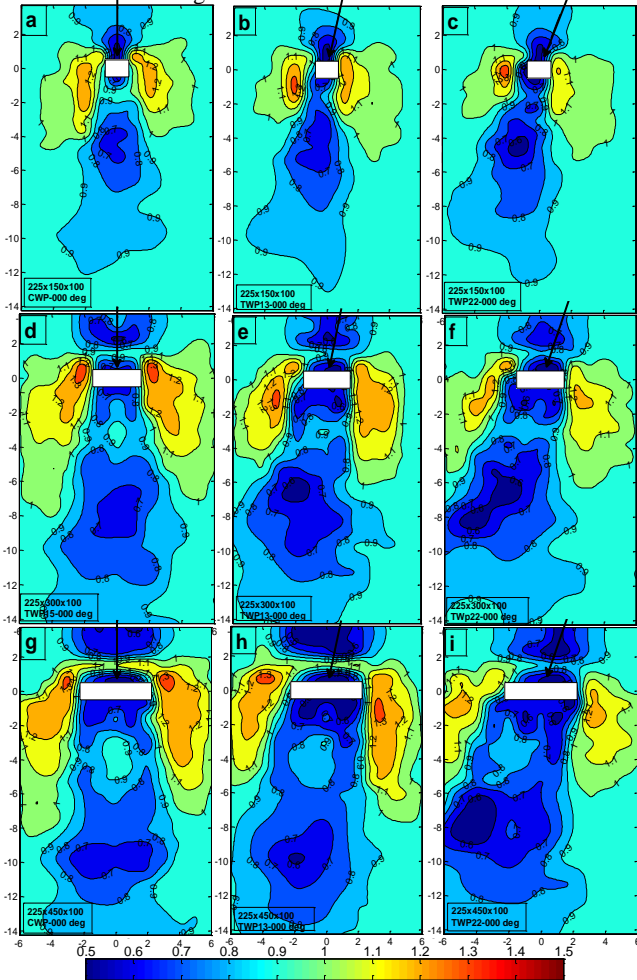


Figure 6. Wind speed ratio distribution at 10 mm above ground around (a) 225×150×100 building with CWP, (b) 225×150×100 building with TWP13, (c) 225×150×100 building with TWP22, (d) 225×300×100 building with CWP, (e) 225×300×100 building with TWP13, (f) 225×300×100 building with TWP22, (g) 225×450×100 building with CWP, (h) 225×450×100 building with TWP13, (i) 225×450×100 building with TWP22.

Model	Deviated angle (°)		
	CWP	TWP13	TWP22
M1	0°	9°	15°
M2	0°	9°	17°
M3	0°	9°	16°
M4	0°	10°	23°
M5	0°	11°	28°

Table 2. Deviation of DFLWS for different building models for three wind profiles CWP, TWP13 and TWP22.

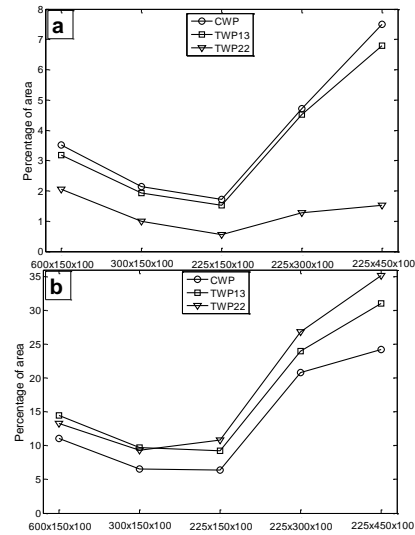


Figure 7. Percentage area of (a) Over-speed ($VR > 1.2$), (b) Sheltered ($VR < 0.8$) resulting from CWP, TWP13 and TWP22.

Conclusions

Five isolated building models with different dimensions were tested in a boundary-layer wind tunnel using both a conventional turbulent boundary layer and two twisted wind profiles to investigate the influence of the twisting effect on the pedestrian-level wind environment. Irwin sensor measurements were converted to velocity ratios (VR) to show the pedestrian-level wind field around different building models. It was found that the DFLWS zone tends to deviate from the exact downstream direction (defined according to the building section) in the twisted wind flow. This deviation is more obvious for short and wide buildings. The over-speed area ($VR > 1.2$) is smaller in the twisted flow than in the conventional turbulent boundary layer flow because the corner streams facing the approaching wind flow is weakened. The sheltered area, on the other hand, increases with the maximum twisted angle exhibited in the twisted profile. The shelter area also increases with the building width due to the interactions with the twisting effect and the front and side faces of the building. The differences in the flow patterns as well as in the distribution of high and low wind speed areas resulted from the use of conventional and twisted profiles suggest that the use of a more realistic approaching wind profile that takes into consideration the topographical influence, i.e. the twisting effect, is necessary to enhance the reliability and accuracy of the assessment of pedestrian-level wind environment around buildings, including Air Ventilation Assessment (AVA) currently employed in Hong Kong.

References

- Flay R.G.L, Vuletich, I.J (1995) Development of a wind tunnel test facility for yacht aerodynamic studies, *Journal of Wind Engineering and Industrial Aerodynamics* 58:231-258
- Hedges K.L, Richards P.J, Mallinson G.D (1996) Computer modelling of downwind sails, *Journal of Wind Engineering and Industrial Aerodynamics* 63:95-110
- Irwin P.A (1981) A simple omnidirectional probe for the measurement of pedestrian level winds. *Journal of Wind Engineering and Industrial Aerodynamics* 7:219-239.
- Tsang C.W, Kwok K.C.S, Hitchcock P.A (2012) Wind tunnel study of pedestrian level wind environment around tall buildings: Effects of building dimensions, separation and podium, *Building and Environment* 49:167-181
- Wu H, Stathopoulos T (1994) Further experiments on Irwin's surface wind sensor, *J. of Wind Engng & Ind Aero.* 53:441-44